The Raman Fingerprints of Quartz, Albite and Calcite

Amelia Carolina Sparavigna

Department of Applied Science and Technology, Polytechnic University of Turin, Italy

Email: amelia.sparavigna@polito.it

Submitted SSRN, October 10, 2023

Abstract

Here we consider a processing method for Raman spectra, suitable to determine the positions of the peaks and their shoulders. This processing is based on the behavior of the first derivative. It can be used as a preprocessing method for a further fitting of the spectrum by means of Tsallis q-Gaussian functions (Sparavigna, 2023). The spectra considered are those of Quartz, Albite and Calcite from RRUFF database.

Keywords: Raman spectroscopy, Tsallis q-Gaussian distribution.

The first use of the term "fingerprint" for Raman spectroscopy, to the best of my knowledge, is in an article published in 1947, about the Raman spectra of hydrocarbons (Fenske et al., 1947). "The basis for applying Raman spectroscopy to hydrocarbon analysis is dependent upon the fact that when a beam of a monochromatic exciting light passes through a transparent medium some of the light is absorbed and may be re-emitted. If this re-emitted light is examined by means of a spectrograph, very weak spectral lines or bands will appear on either side of the line of the exciting light. These weak lines, which are called Raman lines, are characteristic of the substance illuminated and are therefore a "fingerprint" of that substance" (Fenske et al., 1947). From that time on, the points of identification, such as positions of peaks, shoulders and valleys are considered to constitute the characteristic spectral pattern which is defined as the "Raman fingerprint" of a given material.

Fingerprint allows the material classification, "without any preliminary information about composition and structural origin of the individual features" (D'Ippolito, et al., 2015). In this manner, the Raman spectroscopy is used for routine investigations "in materials science, cultural heritage, mineralogy, geology, and gemology and plays an important role also in astromineralogy" (D'Ippolito et al. and references therein; the characterization of materials on Mars is also mentioned).

We have a fingerprint matching when the peak positions are almost the same. In the case that the spectrum has little detail, for instance the spectrum is possessing a few broad peaks with shoulders, a further investigation can be useful and a fitting with components possessing specific line shapes can be relevant. In previous studies (Sparavigna, 2023), we have shown that Tsallis q-Gaussian functions[1], in the symmetric and asymmetric forms, are suitable for being used as line shape of Raman spectral components. In our q-Gaussian analysis, such as in analyses based on other forms of line shapes, the position of the component centers is determined according to the resulting best fits based on iterative procedures. However, iterations can start from initial positions which could be determined, for instance, by the approach here proposed. The spectral data preprocessing that we will describe is based on the first derivative behavior, that is on the "first derivative spectrum" (Mosier-Boss et al., 1995). For spectral comparisons, the proposed processing may be used standalone, that is without any further fitting procedure with components.

The problem of determining the Raman fingerprint seems being requiring further studies, as shown by a recent publication about the Raman spectral mineral classification obtained by means of the

[1] See please the works by Hanel, Tsallis and Umarov mentioned in the References, to appreciate the physical statistics method on which the q-Gaussian functions are based.

Convolutional Neural Network (CNN) (Berlanga et al., 2022). The aim of Berlanga and coworkers is that of having a method which can allow the Martian rovers' instrumentation to automatically identify the minerals. This task is fundamental because of the time delay of communication between Earth and Mars. Berlanga and coworkers also tell that "Most peak detection algorithms identify peaks based solely on amplitude, sacrificing low-amplitude peak detection, and increasing the rate of false positives in low signal to noise situations (Du et al., 2006; Yang et al., 2009). Accordingly, Berlanga et al. used the wavelet space "to simplify peak matching, increase the apparent SNR [signal-to-noise ratio], and bypass baseline removal and peak smoothing steps".

In the Figure 3 of Berlanga et al. we can see that wavelets are identifying five main peaks of Quartz, Albite, Hornblende and Biotite. In this figure, it seems that the range of the Raman shift considered by Berlanga et al. is limited to 800 cm^{-1}, but in their text, it is told the range being from 150 cm^{-1} to 1100 cm^{-1}. Just to understand the range and the peaks we have to deal with, here we consider obtaining the Raman fingerprints of Quartz and Albite from their first derivative spectra. The spectra are provided by the RRUFF database (Lafuente et al., 2015 (the RRUFF database is also used by Berlanga and coworkers). In RRUFF database, a search with Hornblende or Biotite does not provide results. For this reason, we decided to add Calcite as a further example of "Raman fingerprints".

At the web page https://rruff.info/Quartz we can find 10 spectra. R040031, R050125 and R060604 are spectra obtained from oriented samples (we use the processed 0° depolarized data). X080015, X080016, R100134, R110104, R110108, R150074 and R150091 are spectra obtained from unoriented samples (we use the processed data for 532 nm exciting laser).

To determine the position of the peaks, the steps of the algorithm are as follow. 1) A scaling is made to have the spectrum with its maximum intensity at value 1. 2) Data are represented as a function of increasing Raman shift. 3) A "peak" is a part of the spectrum where it has a maximum, then the first derivative of the function is positive before and negative after the peak. 4) The first derivative is taken by the "simple difference" method. 5) If necessary, the spectrum and the first derivative must be smoothed by Savitsky-Golay method. 6) A threshold *t* for the intensity is chosen, so that only the peaks with an intensity above the given threshold are considered. 7) For each intensity peak, the first derivative spectrum has a peak (positive values) and a trough (negative values). The widths of them, a_left and a_right as in the Fig.1, are evaluated. If both a_left and a_right are larger than a given value *w*, the peak of intensity spectrum is considered as a good one. A proper choice of *w* allows reducing the number of false positive. However, other statements based on a_left and a_right can be decided.

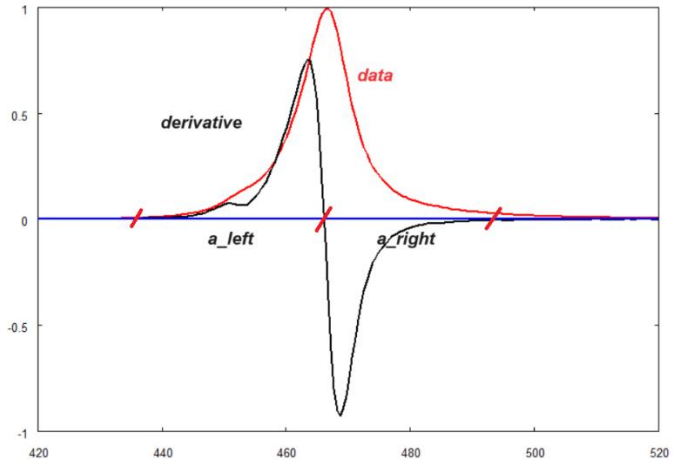

Fig.1: A peak of a Raman spectrum and its first derivative. The derivative has a peak and a trough, positive and negative. The widths, a_left and a_right, are considered as in the figure. Note that a further processing with the second derivative can help in evidencing a small left shoulder of the peak.

Here in the following plots (Figs. 2 and 3) (see all the ten spectra in the Supplementary Figures), the peaks of the **Quartz RRUFF spectra** are shown in the semi log scale. The blue line is representing the intensity threshold.

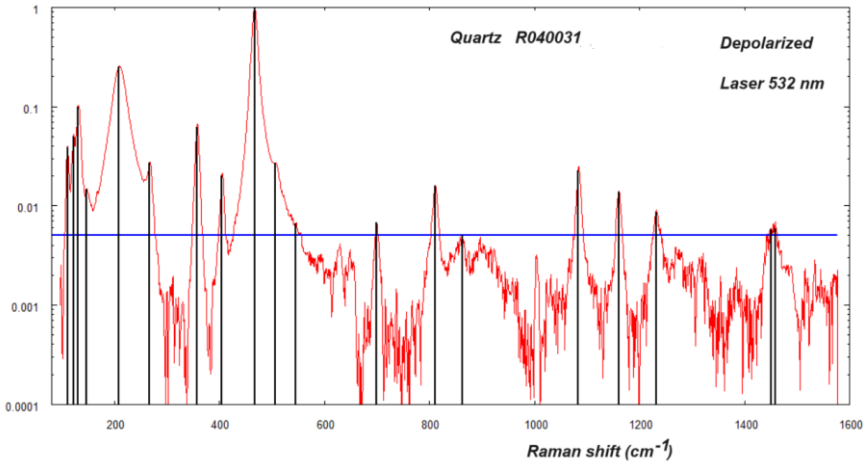

Fig. 2: Intensity threshold at 5/1000.In red the data and in black the position of the peaks as determined by means of the first derivative.

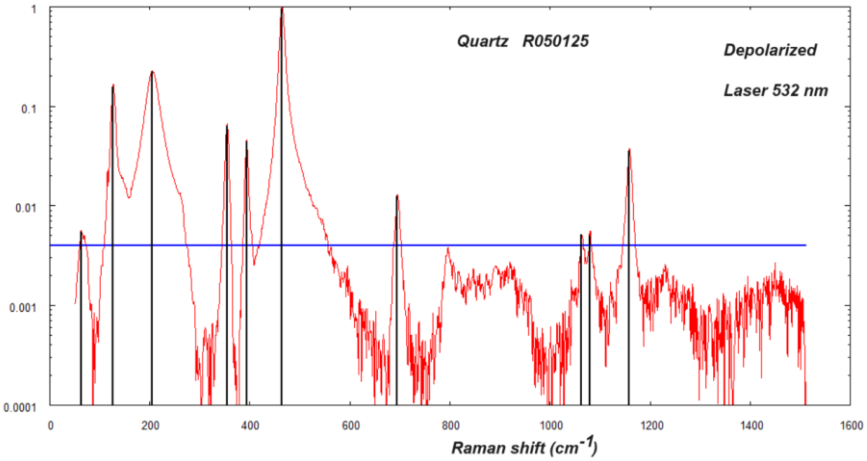

Fig.3: Intensity threshold at 4/1000.

From Figs.2 and 3 and those given in the Supplementary Figures, we can see the data in red. The black lines are the positions of the peaks as given by the first derivative behaviour.

For step 5) of the algorithm, it was told that a smoothing by Savitsky-Golay method is sometime necessary. In the case of Quartz and Calcite, we applied just a very simple smoothing of data, that is (data_s are the smoothed data):

data_s (i) = (data (i+1) + data (i) + data(i-1)) / 3 (*)

For the derivative, it was given as: der(i) = (data_s (i+1) − data_s (i-1)). The smoothing is:

der_s (i) = (der (i-1) + der (i) + der (i+1)) / 3

In the case of Albite, we need for some samples a more complex, that is, a Savitsky -Golay smoothing method. From the analysis of the ten RRUFF spectra, we have the following Table I for Quartz.

	109.6	121.3	130.5	146.5	208.2		265.9		356.4			404.2	466.1	505.7		544.0	698.4	810.2	861.9		1082.8	1159.4	1230.9
62.3			126.0		204.5				353.7		392.9		463.4				694.4			1062.5	1079.1	1158.1	
			129.0	146.9	207.0		264.9		355.5		395.7	403.5	465.4	510.9			701.1	809.9			1082.3	1160.5	
			128.1		204.8		264.1		355.2		394.3	402.9	464.2	516.7			696.5	807.9	1045.1		1081.8	1158.9	
			128.1		204.8		263.6		355.2		394.3	399.1	464.6				695.0	795.9	1065.4			1160.8	
					204.3		264.6		354.8			402.5	464.2	508.1			697.1	808.4			1080.8	1157.5	1228.8
					204.8		264.5		355.2		393.7		464.6	521.5	532.1		696.0	806.0		1070.2		1161.3	1232.6
	109.8	121.4			204.3		265.0		355.7			403.4	464.6	509.0			697.5	808.8			1082.2	1158.9	1230.7
			128.8		206.0	246.9	265.8		356.4		394.5	403.6	465.4	509.2			696.8	809.6			1083.0	1160.6	
			129.8	147.2	206.5		265.3	343.4	356.4	381.9	395.5		465.8	510.2			696.8	798.5		1068.0		1162.5	

Table 1: From top to bottom, peak positions of Quartz R040031, R050125, R060604, X080015, X080016, R100134, R110104, R110108, R150074, R150091 spectra are given (Raman shift in cm^{-1}). The peaks evidenced in red are present in all the spectra. Those evidenced in yellow could be also interesting for further analysis.

Let us consider our Table 1 and compare the peak positions (evidenced in red and yellow) with those given by the Figure 3 by Berlanga et al.: in their figure, the five positions are at about 205, 355, 395, 465 and 695 cm^{-1}. Agreement is evident, but there is a difference. It is in Berlanga et al. peak at 395 cm^{-1} that here we have split in two peaks, which can be both present in some spectra. In the following Table 2, the relative intensities of the five peaks evidenced in red in the previous Table 1 are given.

Spectrum R040031		Spectrum R050125		Spectrum R060604		Spectrum X080015		Spectrum X080016	
Shift	Intensity	Shift	Intensity	Shift	Intensity	Shift	Intensity	Shift	Intensity
208.231	0.252	204.488	0.224	207.006	0.251	204.787	0.258	204.787	0.243
356.365	0.062	353.659	0.063	355.510	0.062	355.207	0.056	355.207	0.030
466.100	0.98	463.352	0.96	465.380	0.96	464.166	0.97	464.648	0.99
698.375	0.007	694.364	0.012	701.117	0.010	696.546	0.009	695.582	0.015
1159.453	0.014	1158.093	0.036	1160.478	0.022	1158.896	0.015	1160.825	0.027

Spectrum R100134		Spectrum R110104		Spectrum R110108		Spectrum R150074		Spectrum R150091	
Shift	Intensity	Shift	Intensity	Shift	Intensity	Shift	Intensity	Shift	Intensity
204.333	0.285	204.754	0.254	204.272	0.332	205.973	0.246	206.455	0.201
354.753	0.072	355.174	0.075	355.656	0.072	356.394	0.080	356.394	0.041
464.193	0.97	464.615	0.98	464.615	0.98	465.352	0.98	465.834	0.97
697.056	0.012	696.031	0.014	697.477	0.017	696.768	0.007	696.768	0.018
1157.478	0.017	1161.273	0.027	1158.863	0.026	1160.564	0.013	1162.493	0.037

Table 2: Peak positions (Quartz) given as Raman shift (cm^{-1}) and relative intensities. Note that the main peak has an intensity close to one. Smoothing by (*) was just slightly affecting the peak intensities.

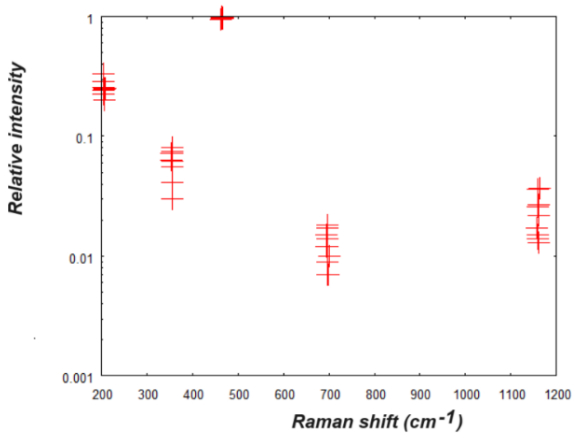

Fig.4: Plot of data in Table 2 (semi log scale).

Table 1 and Table 2 are representing the "fingerprints" of Quartz, as made by positions and relative intensities. We can decide to use just five peaks, or add further details from the Tables, increasing the number of peaks with their relative intensities too. To these two tables, we could also add details about asymmetries, by means of a_left and a_right parameters.

Let us consider some of the **Albite spectra given by RRUFF**, at the following link https://rruff.info/albite/display=default/ . The spectra analysed are: R040068 (laser 532 nm, depolarized), X050127 (laser 785nm, unoriented), R050253 (laser 532 nm, depolarized), R050402 (laser 532 nm, depolarized), R060054 (laser 532 nm, unoriented), R070268 (laser 532 nm, depolarized), R100169 (laser 532 nm, unoriented), R230008 (laser 532 nm, depolarized, unoriented). Here in the following we will show two Albite spectra (all the eight spectra are given in the Supplementary Figures). For three of the Albite spectra, we did the same smoothing of Quartz; for the other spectra, the smoothing was more consistent (Savitsky-Golay method) and therefore the plots provide the data (in red) and the corresponding smoothed curve (in black).

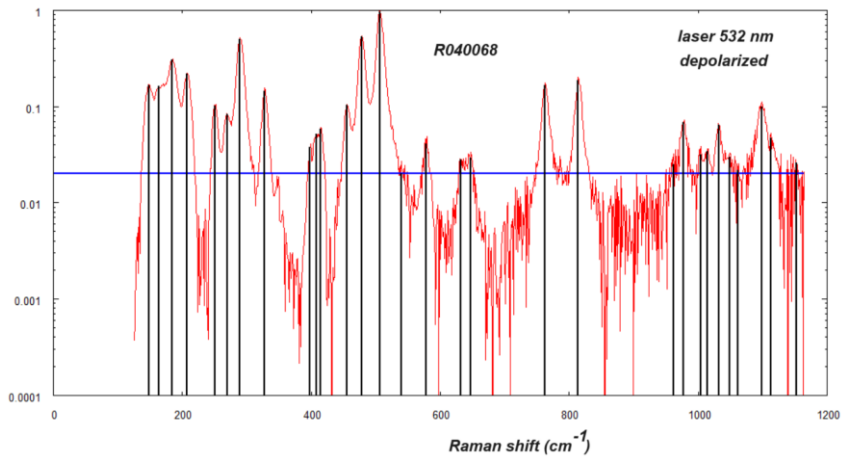

Fig.5: Intensity threshold at 20/1000, with the same smoothing approach (*) used for Quartz and Calcite.

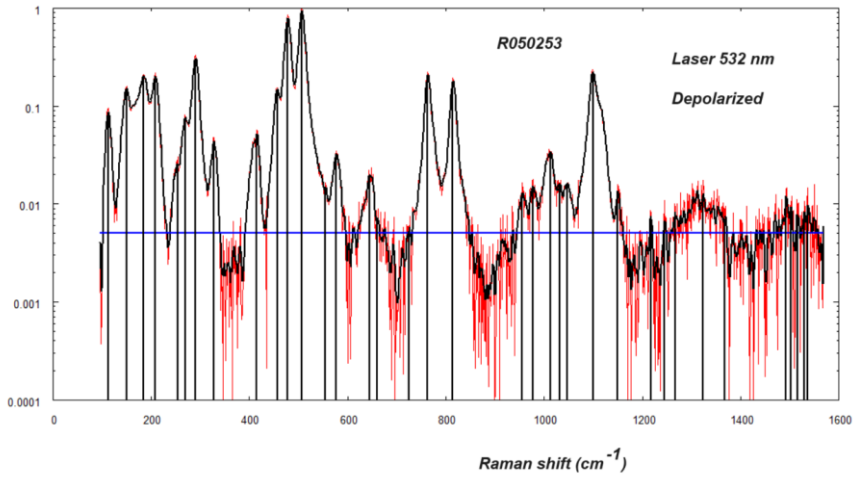

Fig.6: Intensity threshold at 5/1000. In red the data and in black the curve of the smoothed data (smoothing Savitsky-Golay method).

The Albite spectra seem being more complex than those of Quartz. Here in the following Table the Albite peaks are given, as we did for Quartz in Table I.

First part, from 100 to 610 cm^{-1}

	147.4	163.4	184.1	206.9		250.1	269.3	289.1	327.2	397.5	407.6	414.2	455.2	477.9	505.8	539.0	577.9		
							251.0		286.0	320.0	367.0	407.0		445.0	479.0	509.0	551.0	565.0		607.0
110.7	148.9		183.2	206.4		252.7	268.4	289.0	326.5				414.0	455.7	477.1	505.5	552.6	576.1		
	153.8	163.6	185.6	208.8	234.4			291.4	330.1	350.5			410.4	459.3	479.5	507.9			594.9	
		168.6						281.4		383.1	404.3				474.2	510.9		569.2		
			178.1	199.8				286.6	329.5		409.5				479.4	506.9		570.5		
112.5		163.7	185.1	208.6		250.9	270.3	290.1	328.8		408.2	414.4	457.3	479.2	507.4			579.0		
		161.9	185.0	208.7		252.1	270.4	290.6	309.4	328.7	408.3	416.0			478.7	507.1		578.5		

Second part, from 610 to 900 cm^{-1}

	631.1		646.1								762.2			813.6					
	629.0					681.0	710.0		736.0			772.0	794.0	809.0	834.0		873.0		
			643.9	659.0				723.8		761.7				813.2					
	625.2		647.4						731.8	762.9				812.0		855.2			
	631.9	638.6	642.5			717.7						774.1	786.1						
	630.3		642.9					723.9		763.9				809.2		855.6	876.2		
			647.4							763.9				815.6	839.1				
	633.4		644.5			717.3	720.7			763.6				814.7					

Third part, from 910 to 1160 cm^{-1}

			960.7	977.1		1003.4	1014.0	1031.4		1048.2	1061.3	1097.8		1112.0		1151.4			
	918.0	940.0		977.0	987.0		1013.0	1037.0		1050.0		1090.0		1112.0	1128.0	1146.0			
			954.4	975.7			1011.3	1030.2		1045.7		1098.6				1149.0			
	909.5		961.1	977.9	982.4	1002.4	1013.6	1030.2				1099.7				1147.9	1155.6		
							1019.5	1032.5				1094.7	1104.8	1115.4					
901.8	922.0	937.0	961.5		985.2		1011.7	1034.3		1044.0	1063.8	1098.5	1101.8			1152.9	1155.4		
				980.6			1016.1	1034.4		1047.0		1100.8				1150.9			
				977.6			1013.8	1031.6	1033.1	1044.7		1098.7				1149.8			

Table 3: From top to bottom, peak positions of Albite R040068, X050127, R050253, R050402, R060054, R070268, R230008, R100169 spectra are given (Raman shift in cm^{-1}). The peaks evidenced in red are present in all the spectra. Those evidenced in yellow could be also interesting for further analysis.

Table 3 is representing the positions of the "fingerprints" of Albite. Let us compare the results given by this Table with the data provided by Berlanga et al., 2022. From the Figure 3 by Berlanga and coworkers we have the five peaks evidenced by wavelets at positions 285, 410, 505, 625, 720 cm^{-1}. Agreement

exists for the two peaks at 285 and 505 cm^{-1}. For the other peak positions given by Berlanga and coworkers, we must consider them as an average of the positions given in our Table 3.

As for quarts, we could also add the relative intensity. Note that, in the case of Albite, we have six peaks which are present in the eight spectra. However, the number could change if all the spectra provided by RRUFF are considered.

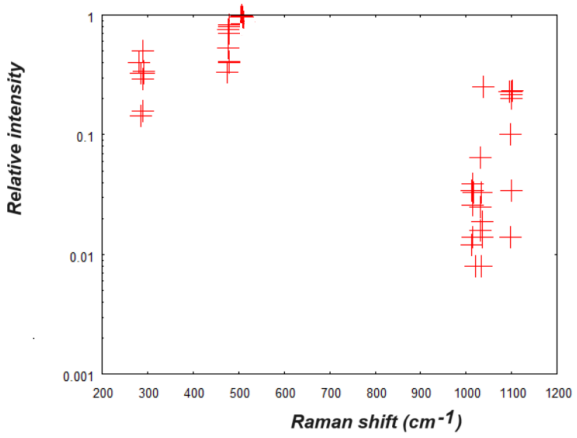

Fig.7: Relative intensities of the six peaks which are present in the eight Albite sample (semi log scale).

Let us pass to analyse the **Calcite spectra**, https://rruff.info/calcite/display=default/ . Samples are R040070 (laser 532 nm, depolarized), R040170 (laser 532 nm, depolarized), R050048 (laser 532 nm, depolarized), R050009 (laser 532 nm, depolarized), R050127 (laser 532 nm, depolarized), R050128 (laser 532 nm, unoriented), R050130 (laser 532 nm, depolarized), X050034 (laser 785 nm, unoriented), X050035 (laser 785 nm, unoriented), R050307 (laser 532 nm, depolarized), R150020 (laser 532 nm, unoriented), and R150075 (laser 532 nm, unoriented).

In the case of Calcite we use the smoothing (*) for all the spectra. However, after this smoothing we had to rescale the data once more, to have the intensity maximum to value 1. Here in the following figures, two of the Calcite spectra are shown (all the spectra in the Supplementary Figures).

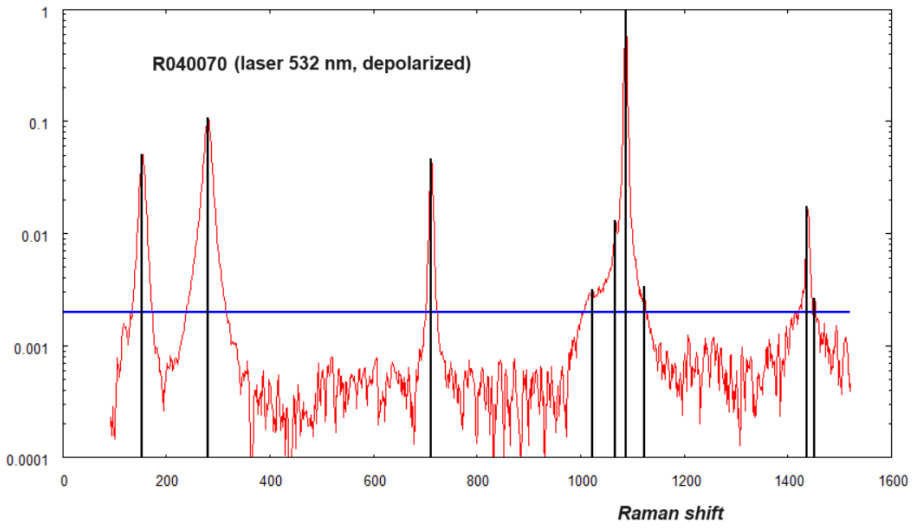

Fig. 8: Intensity threshold 0.002 .

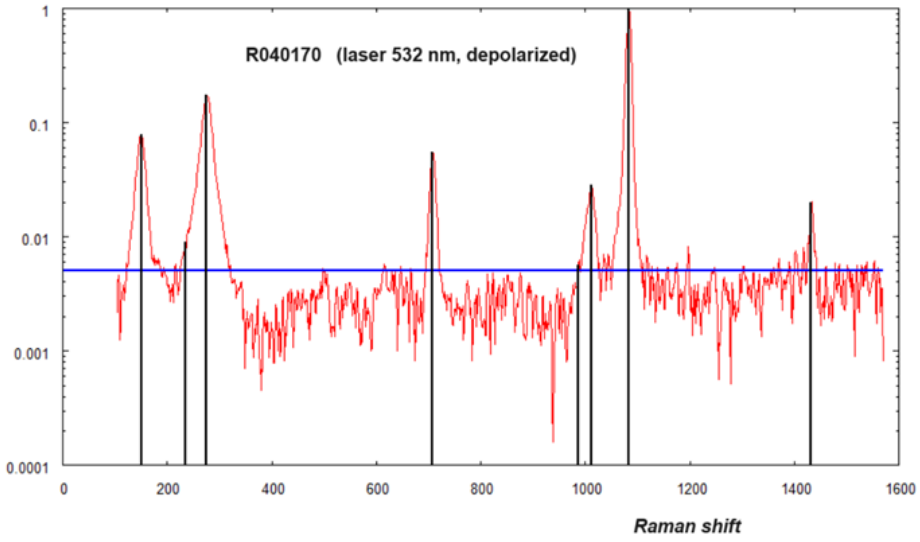

Fig. 9: Intensity threshold 5/1000.

		153.1			280.9			711.8		1022.3		1067.2	1087.0	1122.9		1437.6	1451.8
		150.1	234.4		275.7			707.6	986.8	1011.3			1083.2			1432.5	
119.2		155.4			282.1			711.9				1066.6	1085.1	1120.9		1434.0	1452.9
		156.3			281.3			719.9				1068.9	1086.6		1262.5	1435.5	
		157.9			284.3			715.0				1069.0	1088.9			1439.4	
113.6		156.6						713.7		1019.2	1045.5	1069.0	1087.6			1438.2	
			217.0		282.0	428.0	575.0	712.0		1018.0		1066.0	1085.0			1435.0	
		152.5			278.1			709.9				1064.5	1084.3			1433.5	
117.7	124.5	156.3		273.5	281.7			713.6			1062.2	1068.5	1087.8				
		156.8			282.6		701.6	713.2		1014.0	1020.3	1068.0	1087.8	1113.3			

Table 4: From top to bottom, positions of the peaks (in cm^{-1}) of R040070, R040170, R050048, R050009, R050127, R050130, X050034, R050307, R150020 and R150075.

181.6 191.8 207.7 250.1 281.4 702.8 706.2 854.2 1061.0 1086.6

214.0 282.0 437.0 453.0 712.0 955.0 964.0 979.0 1085.0 1125.0 1187.0 1301.0 1391.0 1435.0 1461.0 1471.0

Table 5: Peak positions (in cm^{-1}) of R050128 and X050035.

As we did for Quartz and Albite, further information for the Raman fingerprint can be provided by the relative intensity. In the case of Calcite, we consider all the peaks evidenced by the algorithm and given in the previous Tables 4 and 5. The result is shown in the following plot.

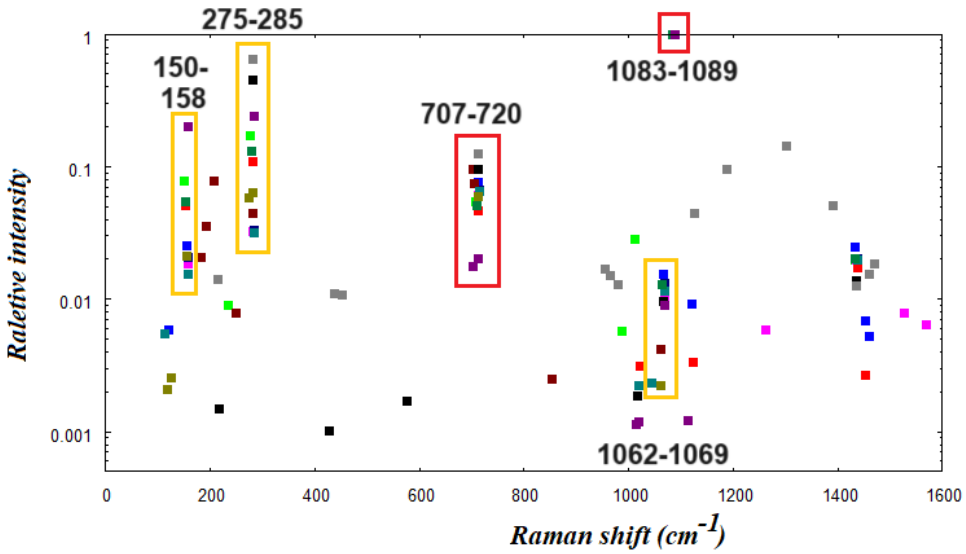

Fig. 10. Relative intensities for the peaks given in the Table 4 and 5.

Further studies are planned for testing algorithm and any possible improvement of it.

References

1. Berlanga, G., Williams, Q., & Temiquel, N. (2022). Convolutional neural networks as a tool for Raman spectral mineral classification under low signal, dusty Mars conditions. Earth and Space Science, 9(10), e2021EA002125.
2. D'Ippolito, V., Andreozzi, G. B., Bersani, D., & Lottici, P. P. (2015). Raman fingerprint of chromate, aluminate and ferrite spinels. Journal of Raman Spectroscopy, 46(12), 1255-1264.
3. Du, P., Kibbe, W. A., & Lin, S. M. (2006). Improved peak detection in mass spectrum by incorporating continuous wavelet transform-based pattern matching. Bioinformatics, 22(17), 2059–2065.
4. Fenske, M. R., Braun, W. G., Wiegand, R. V., Quiggle, D., McCormick, R., & Rank, D. H. (1947). Raman spectra of hydrocarbons. Analytical Chemistry, 19(10), 700-765.
5. Hanel, R., Thurner, S., & Tsallis, C. (2009). Limit distributions of scale invariant probabilistic models of correlated random variables with the q-Gaussian as an explicit example. The European Physical Journal B, 72(2), 263.
6. Lafuente, B., Downs, R. T., Yang, H., & Stone, N. (2015). 1. The power of databases: The RRUFF project. In Highlights in mineralogical crystallography (pp. 1-30). De Gruyter (O).
7. Mosier-Boss, P. A., Lieberman, S. H., & Newbery, R. (1995). Fluorescence rejection in Raman spectroscopy by shifted-spectra, edge detection, and FFT filtering techniques. Applied Spectroscopy, 49(5), 630-638.
8. Savitzky, A., & Golay, M. J. (1964). Smoothing and differentiation of data by simplified least squares procedures. Analytical chemistry, 36(8), 1627-1639.
9. Sparavigna, A. C. (2023). q-Gaussian Tsallis Line Shapes and Raman Spectral Bands. International Journal of Sciences, 12(03), 27-40. http://dx.doi.org/10.18483/ijSci.2671
10. Sparavigna, A. C. (2023). q-Gaussian Tsallis Functions and Egelstaff-Schofield Spectral Line Shapes. International Journal of Sciences, 12(03), 47-50. http://dx.doi.org/10.18483/ijSci.2673

11. Sparavigna, A. C. (2023). q-Gaussian Tsallis Line Shapes for Raman Spectroscopy (June 7, 2023). SSRN Electronic Journal. http://dx.doi.org/10.2139/ssrn.4445044
12. Sparavigna, A. C. (2023). Formamide Raman Spectrum and q-Gaussian Tsallis Lines (June 12, 2023). SSRN Electronic Journal. http://dx.doi.org/10.2139/ssrn.4451881
13. Sparavigna, A. C. (2023). Tsallis and Kaniadakis Gaussian functions, applied to the analysis of Diamond Raman spectrum, and compared with Pseudo-Voigt functions. Zenodo. https://doi.org/10.5281/zenodo.8087464
14. Sparavigna A. C. (2023). Tsallis q-Gaussian function as fitting lineshape for Graphite Raman bands. ChemRxiv. Cambridge: Cambridge Open Engage; 2023.
15. Sparavigna A. C. (2003). Fitting q-Gaussians onto Anatase TiO2 Raman Bands. ChemRxiv. Cambridge: Cambridge Open Engage; 2023.
16. Sparavigna, A. C. (2023). SERS Spectral Bands of L-Cysteine, Cysteamine and Homocysteine Fitted by Tsallis q-Gaussian Functions, International Journal of Sciences 09(2023):14-24 DOI: 10.18483/ijSci.2721
17. Sparavigna, A. C. (2023). Asymmetric q-Gaussian functions to fit the Raman LO mode band in Silicon Carbide. ChemRxiv. http://dx.doi.org/10.26434/chemrxiv-2023-f8gk3
18. Tsallis, C. (1988). Possible generalization of Boltzmann-Gibbs statistics. Journal of statistical physics, 52, 479-487.
19. Tsallis, C. (1995). Some comments on Boltzmann-Gibbs statistical mechanics. Chaos, Solitons & Fractals, 6, 539-559.
20. Umarov, S., Tsallis, C., Steinberg, S. (2008). On a q-Central Limit Theorem Consistent with Nonextensive Statistical Mechanics. Milan J. Math. Birkhauser Verlag. 76: 307–328. doi:10.1007/s00032-008-0087-y. S2CID 55967725.
21. Yang, C., He, Z., & Yu, W. (2009). Comparison of public peak detection algorithms for MALDI mass spectrometry data analysis. BMC Bioinformatics, 10, 1–13.

The Raman Fingerprints of Quartz, Albite and Calcite: Supplementary Figures

Amelia Carolina Sparavigna

Department of Applied Science and Technology, Polytechnic University of Turin, Italy

Email: amelia.sparavigna@polito.it

Submitted SSRN, October 10, 2023

The following plots are showing the **ten Quartz RRUFF spectra in RRUFF database, link** https://rruff.info/quartz/display=default/ . The plots are given in the semi log scale. The blue line is representing the intensity threshold.

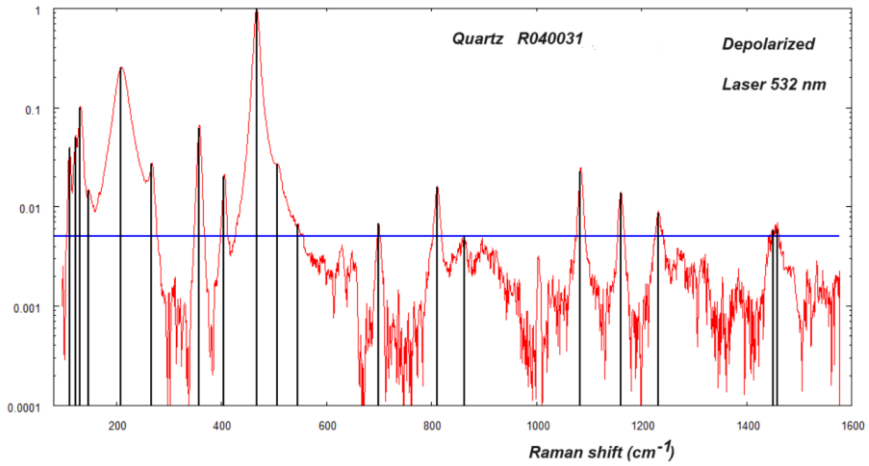

Intensity threshold at 5/1000.In red the data and in black the position of the peaks as determined by means of the algorithm based on the first derivative.

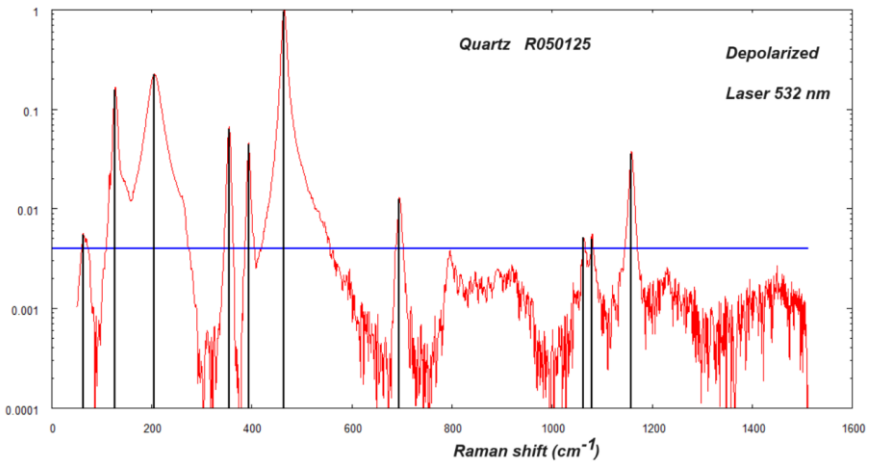

Intensity threshold at 4/1000.

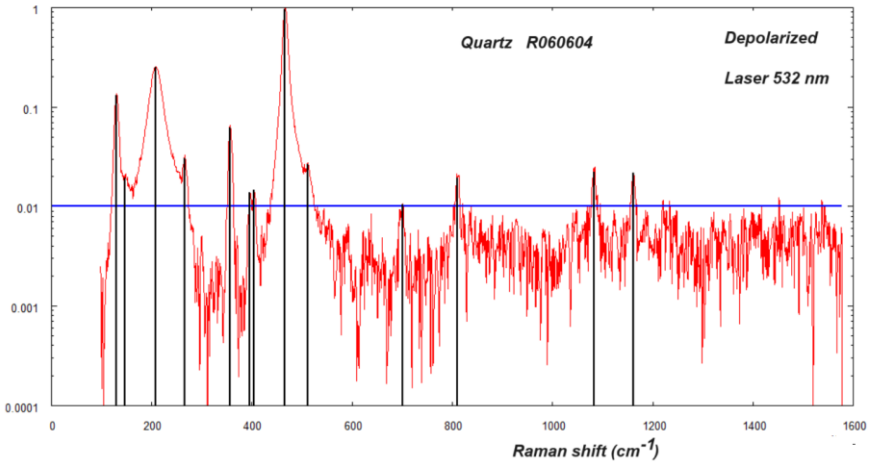

Intensity threshold at 10/1000.

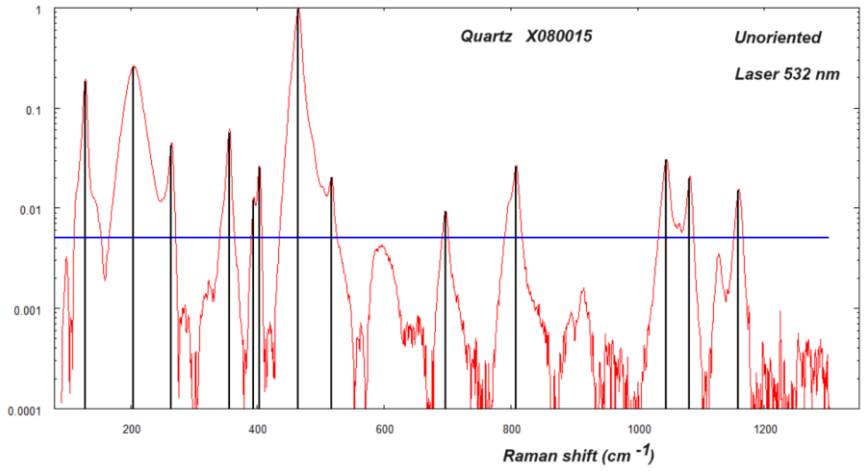

Intensity threshold at 5/1000.

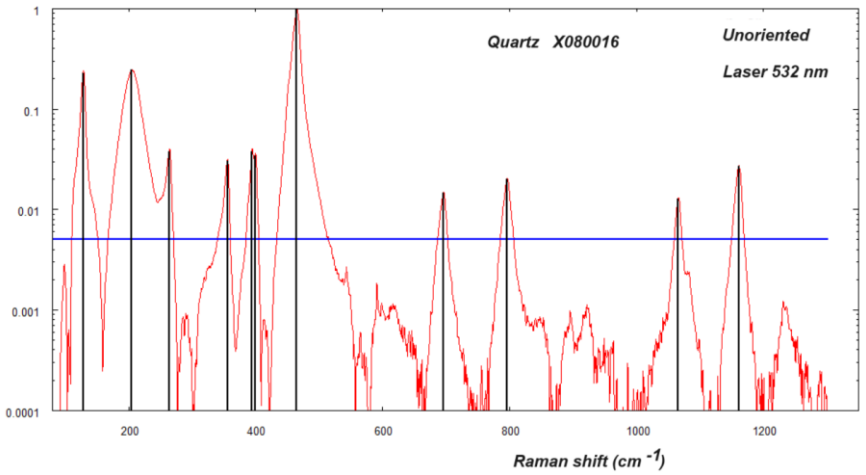

Intensity threshold at 5/1000.

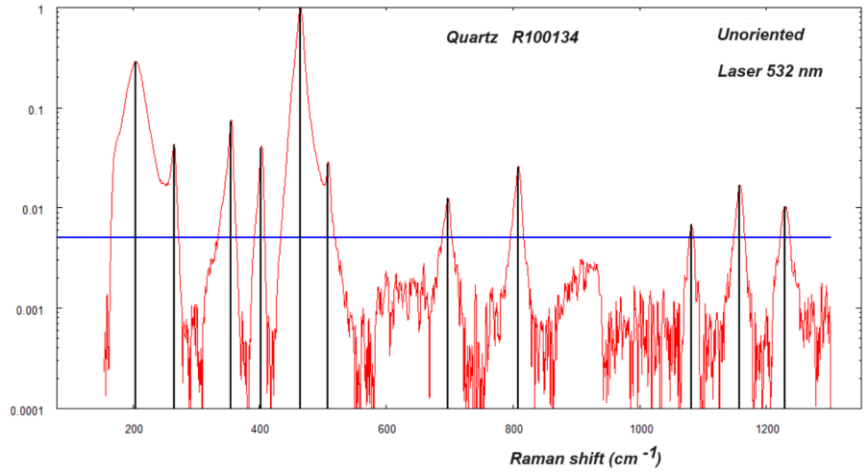

Intensity threshold at 5/1000.

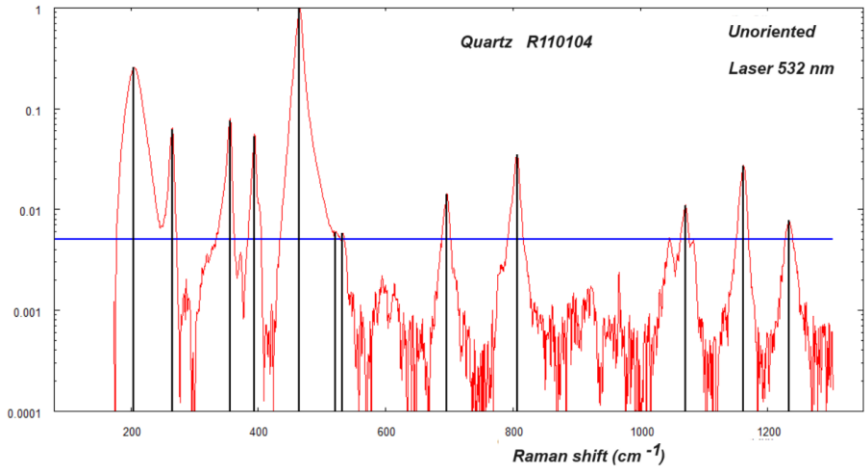

Intensity threshold at 5/1000.

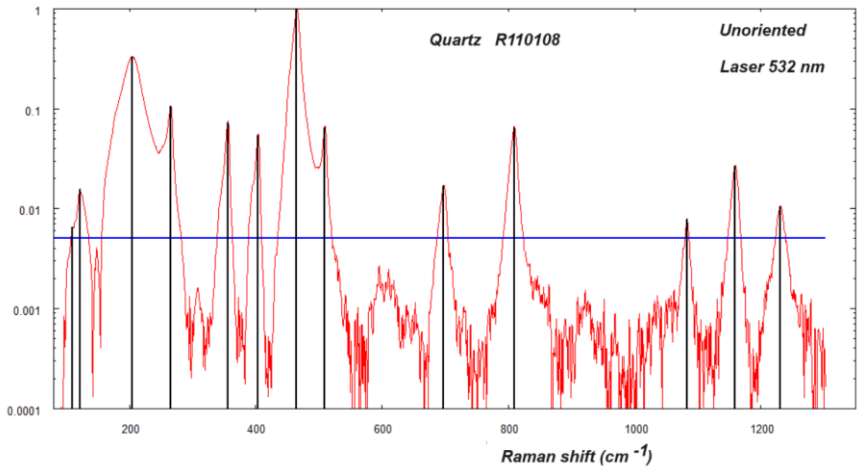

Intensity threshold at 5/1000.

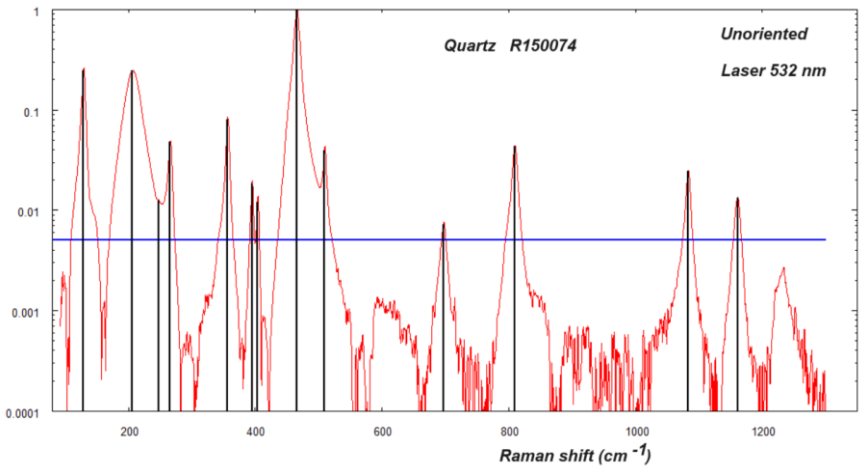

Intensity threshold at 5/1000.

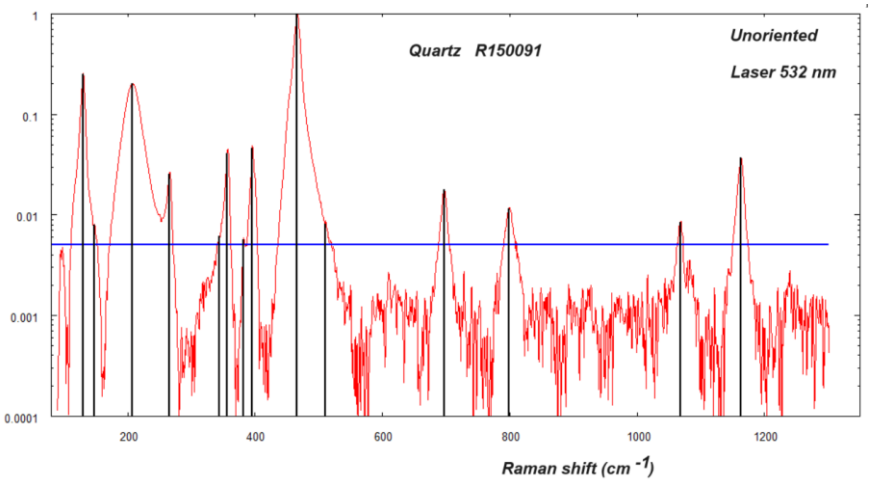

Intensity threshold at 5/1000.

The black lines are the positions of the peaks as given by the first derivative behaviour.

Eight Albite spectra, chosen from the RRUFF database at https://rruff.info/albite/display=default/ given in the following plots (semi log scale).

For three of the Albite spectra, we did the same smoothing of Quartz; for the other spectra, the smoothing was more consistent (Savitsky-Golay SG method) and therefore the plots provide the data (in red) and the corresponding smoothed curve (in black).

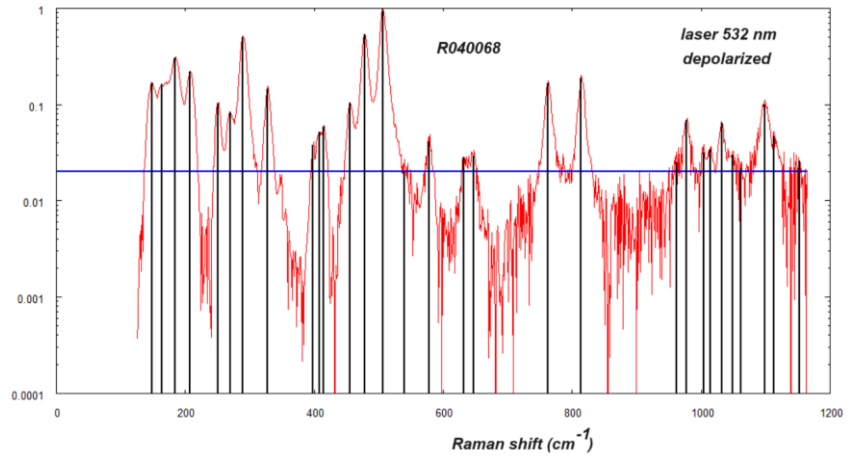

Intensity threshold at 20/1000.

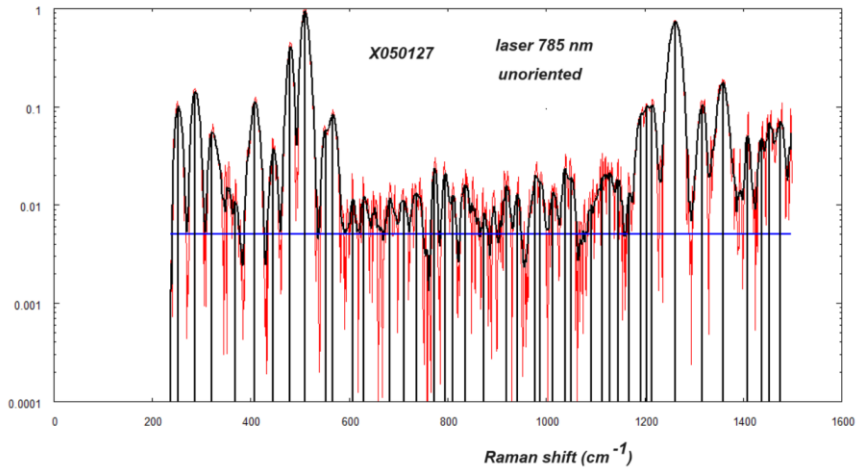

Intensity threshold at 5/1000. In red the data and in black the curve of the SG smoothed data.

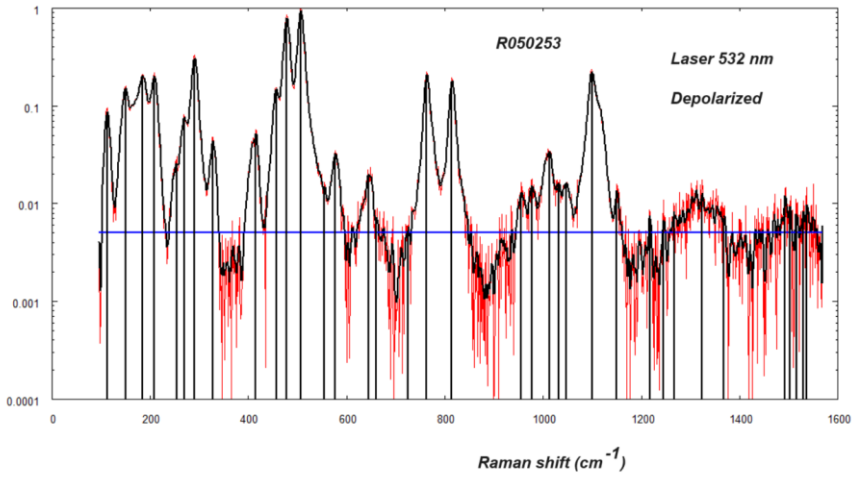

Intensity threshold at 5/1000. In red the data and in black the curve of the SG smoothed data.

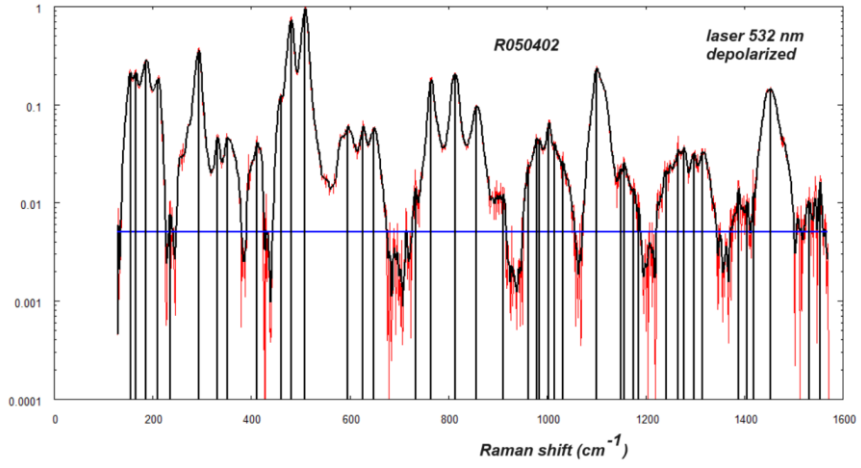

Intensity threshold at 5/1000. In red the data and in black the curve of the SG smoothed data.

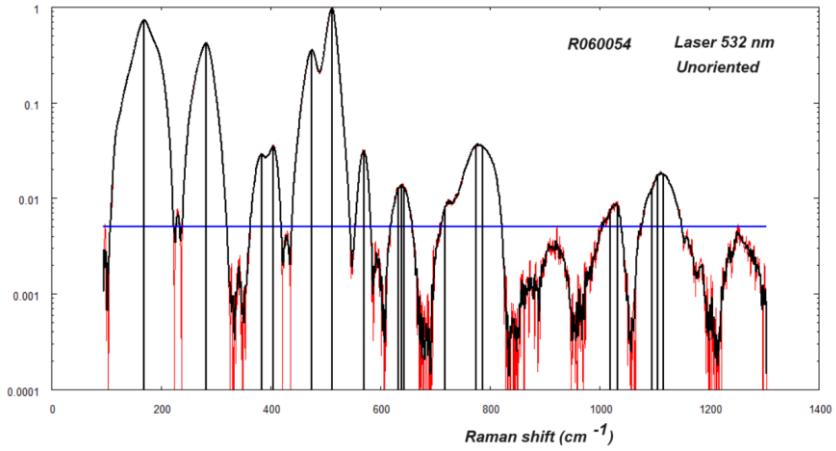

Intensity threshold at 5/1000. In red the data and in black the curve of the SG smoothed data.

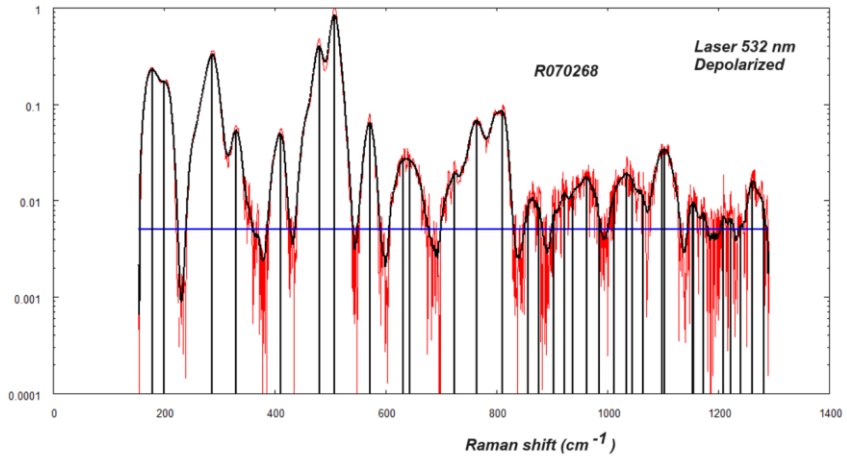

Intensity threshold at 5/1000. In red the data and in black the curve of the SG smoothed data.

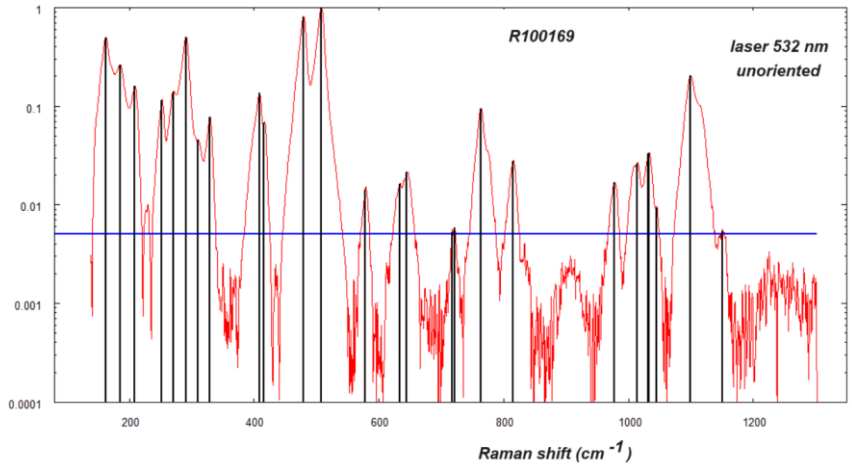

Intensity threshold at 5/1000.

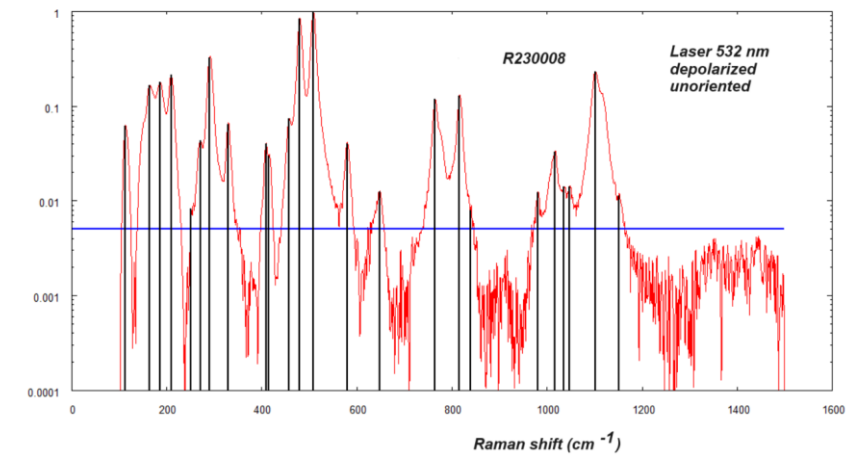

Intensity threshold at 5/1000.

Calcite RRUFF spectra

Available at https://rruff.info/calcite/display=default/

For the Calcite spectra, we did the same smoothing of Quartz.